J Am Oil Chem Soc (2011) 88:773–783
DOI 10.1007/s11746-010-1721-8

ORIGINAL PAPER

Investigation of Chocolate Surfaces Using Profilometry and Low Vacuum Scanning Electron Microscopy

Hanna Dahlenborg · Anna Millqvist-Fureby · Björn Bergenståhl · Daniel J. E. Kalnin

Received: 7 July 2010 / Revised: 1 November 2010 / Accepted: 13 November 2010 / Published online: 30 November 2010

Abstract In this study we establish the use of optical non-contact profilometry combined with low vacuum scanning electron microscopy (LV SEM) for the investigation of lipid surfaces. We illustrate, by using profilometry, a methodology for investigation of chocolate surface topology as a function of time, in the same area of interest. Both qualitative and quantitative data analysis has been performed for profilometry data. Further, relating these results to LV SEM images provides complementary topological information and hence a useful toolkit for the study of the chocolate surface prior and post fat bloom formation. For the demonstration of the successful combination of these two analytical techniques, white chocolate pralines were stored at two temperature-controlled conditions (at 18 °C, and cycled between 15 and 25 °C). Surface properties were then investigated during 36 weeks of storage. The surface images and the roughness parameters indicated distinct development of surface characteristics for the two storage conditions. From the results it is suggested that some imperfections, in the form of pores or protrusions, could play a role in fat bloom development and that there may be different main mechanisms of fat migration taking place for the different storage environments. In the present work, a positive correlation of profilometry data to chocolate surface characteristics and early bloom development has been established. There are indications that early prediction of fat bloom can be possible, however further work needs to be done to quantify prediction of fat bloom.

Keywords Chocolate · Surface structure · Surface topology · Roughness · Waviness · Fat bloom · Oil migration · Scanning electron microscopy · Optical profilometry

H. Dahlenborg · A. Millqvist-Fureby · D. J. E. Kalnin (✉)
YKI, Institute for Surface Chemistry, Box 5607,
114 86 Stockholm, Sweden
e-mail: daniel.kalnin@yki.se

H. Dahlenborg · B. Bergenståhl
Department of Food Technology, Engineering and Nutrition,
Lund University, P.O. Box 124, 221 00 Lund, Sweden

Introduction

Chocolate is a confection defined by its raw materials: sugar, cocoa mass, cocoa butter (CB), and milk solids in the case of milk or white chocolate. However, from a material science perspective, chocolate is a composite material consisting of solid particles (i.e. cocoa powder, sugar and in some cases milk powder) in a lipid continuous matrix, where the final quality of the product is highly dependent on the polymorphic forms of the triacylglycerols (TAG) in the fat phase and the distribution and size of the solid particles therein.

Chocolate is unique in that it is solid at room temperature and at the same time melts easily in the mouth. This property of chocolate is due to the lipid matrix, consisting mainly of CB, which has a relatively simple TAG composition that is responsible for a specific polymorphism (formation of different crystalline structures with the same composition) [1, 2]. CB TAG can crystallize into six different polymorphs which can be named as form I–VI [3] or as γ, α, β'_2, β'_1, β_2 and β_1 [4], with respect to increasing stability and increasing melting points from approximately 17–36 °C. However, more recent research by Van Malssen et al. [5] found only five polymorphic forms, where β' existed as a phase range rather than two distinct separate phases. Further recent studies have advanced the

understanding of the CB structure and its individual TAG [6–8]. Still, the former mentioned nomenclatures are often used in the field of chocolate research and chocolate industry. Form V is the desired form for TAG in chocolate, achieved when it is well tempered (controlled crystallization) during production, while form VI is a thermodynamically stable polymorph, normally associated with fat bloom.

Chocolate that has developed fat bloom is normally characterized by loss of its initial gloss and the greyish/whitish haze formed at the surface. This dulling appearance of fat bloom is generally explained by the scattering of light of the needle-like fat crystals that are formed at the chocolate surface [9]. However, fat bloom can also take various other forms, from surface to internal structures, depending on the product and the storage conditions [1, 10–13]. Fat bloom makes the chocolate appear unappetizing and is thereby a major issue that leads to rejection and to reduced shelf-life in chocolate, particularly in filled chocolate products such as pralines.

Fat bloom on center-filled chocolate products is mostly thought to consist of diluted or melted CB that migrates to the chocolate surface, where it re-crystallizes into the most stable polymorphic form, VI [14, 15]. Still, the mechanism of fat migration in chocolate pralines is not yet fully understood, and hence the detailed development of fat bloom remains unclear. However, the most cited mechanism by which CB migrates to the surface of filled chocolate has been fat diffusion, where a diffusion equation derived from Fick's second law normally is used to model the migration [16, 17]. The diffusive mobility in the mainly crystalline matrix can be expected to depend on the exchange rate at the liquid crystal interfaces as suggested by Löfborg et al. [18]. Lately, also capillary flow has been claimed to play a major role [19–21]. In a hypothesis paper by Aguilera et al. [21] it is proposed that within the chocolate matrix, formed by an assembly of fat-coated particles, the liquid fraction of CB (which increases with temperature) is likely to move under capillary flow through interparticle passages and connected pores.

The relationship between surface topology and fat migration has been investigated by some researchers, where atomic force microscopy, scanning electron microscopy and laser scanning microscopy have been used as the main techniques [13, 22–28]. Some of these studies have reported chocolate surfaces featuring imperfections in form of pores and protrusions, which could be related to fat migration and fat bloom formation. Smith and Dahlman [27] suggested that bloom growth in pralines is a two-step process, with drops initially forming at the surface and then bloom crystals nucleating and growing from them. In agreement with this study, Sonwai and Rousseau [28] found that cone-like structures at the surface of milk chocolate might have formed by welling and deposition of liquid-state fat pushed from within the matrix onto the surface during contraction. These cones hardened with age, and crystal outcroppings protruded from the cones. In addition, the presence of a porous structure within chocolate has been shown by mercury porosimetry, and formation of fat bloom was related to these pores [29].

Optical profilometry, a white light interferometry technique, has been used in various fields in order to characterize surface topology of materials [30–32]. However, it is a technique not widely used in the field of food technology. Based on a certain set of statistical parameters, derived from a surface profile or a surface map, the surface topology can be quantified. Since these analyses can be performed using a non-contact mode, surface damage will be avoided. Although some research has been devoted to studying the development of surface topology on fresh and bloomed chocolate, rather less attention has been paid to studying the change of these topological features in a specific area over time.

The aim of this study is to follow the development and kinetics of surface topology in a specific area as a function of time and storage temperature. This will be realized by employing optical profilometry. Further, by combining this technique with low vacuum scanning electron microscopy (LV SEM), we can gain insight in the mechanisms taking place during migration of oil from the filling to the chocolate surface. Understanding the role of chocolate surface topology development over time can lead to deeper understanding of the mechanism of fat migration and thus, also an extended understanding of the early stages of fat bloom on chocolate. Different ways of detecting, preventing and controlling the growth of fat bloom can then be further envisaged.

Materials and Methods

Materials

White chocolate pralines with a hazelnut filling were manufactured by Ganache AB (Lilla Edet, Gothenburg, Sweden). The composition of the white chocolate and the hazelnut filling is listed in Table 1. The hazelnut mass consisted of caramelized and mixed hazelnuts, the milk chocolate had a cocoa level of 40% and contained whole milk powder, and the cream in the filling contained 40% fat. The white chocolate was tempered in a tempering unit (LCM 25 Twin), with temperatures set to 43.0 and 28.5 °C.

The selection of white chocolate for analysis was based on a parallel study where Confocal Raman Microscopy was used as the main technique. Because of interfering fluorescence when analyzing milk- and dark chocolate (probably due to the cocoa solids) white chocolate was the most

Table 1 Composition of white chocolate and hazelnut filling

	White chocolate	Hazelnut filling
Cocoa butter (%)	35	
Sugar (%)	43	
Whole milk powder (%)	21.5	
Emulsifier and vanilla (%)	0.5	
Hazelnut mass (%)		54
Cream (%)		27
Milk chocolate (%)		19
Total fat (%)	41.1	36.1
Sugar (%)	43	31.4
Water (%)	<1	15

suitable option. Still, the methods used in this study are applicable to the same extent for dark chocolate.

Storage Conditions

Five days after production, the samples were stored at two different temperature-controlled environments. The samples were stored in heating cabinets (temperature accuracy ±0.5 °C) where the temperature was kept at either 18 °C or cycled between 15 and 25 °C, with a temperature ramp of 0.1 °C/min and a residence time at each temperature of 12 h (±2 h). The actual temperature was additionally controlled by a k-type thermocouple using a Picco Tc-08 interface for continuous measurement. The samples were stored for 36 weeks in these temperature-controlled environments, with the exception that the cycled samples were transferred to 18 °C after the 12th week. This was due to the initial intention of ending the study after 12 weeks storage.

Profilometry

Instrumentation

The surface topology of the chocolate was analyzed using Profilometry Zygo New View 5010 (Middlefield, CT, USA), which is a non-contact profilometry method based on white light interferometry. Light from the microscope is divided within the interferometric objective: one portion is reflected from the sample surface and another portion reflects from an internal, high quality reference surface in the objective. Both portions are then directed into a CCD camera. Interference between the two light beams results in an image of light and dark bands, fringes, which characterize the surface structure of the sample observed. The surface is scanned by vertically moving the objective with a piezoelectric transducer. As the objective scans, a video system captures intensities at each camera pixel. These intensities are converted into images by a software application. The results are displayed on a color display as images, plots, and numeric representations of the surface. Since profilometry uses reflective light, the degree of light absorption to the analyzed sample has no impact on the results. Therefore, this technique is also applicable to dark chocolate and other light absorbing surfaces.

Limitations for this technique are that the sample reflectivity must be high enough (better than 0.1%), the roughness (peak-to-valley) should be <100 μm and the local inclination of the topological features should not be too steep, in this case the inclination should be <15°. The *number of points* displays the number of valid data points in the data set, i.e. the number of camera pixels used in the analysis. Without data drop out the value will be 307×10^3 points. Thus, due to topological surface features with high inclinations (>15°), some profilometry data might not be interpretable and will then be illustrated with black color in the result images [33, 34].

In order to quantify the surface topology, there is access to several surface topological parameters, and in order to obtain reliable results it is essential to choose appropriate ones. *Peak number* (peaks per observation area) is the peak count or the number of peaks included in the analysis. A peak is defined as a data point whose height is above an operator-selected bandwidth. The band is centered around the mean plane of the data, where the upper edge of the band is the reference value for finding peaks. Thus, it is of importance that the choice of reference values is well considered. *Peak height* (μm) is the height for each peak included in the peak analysis and *peak area* (μm^2) is the area of each peak included in the peak analysis. The roughness parameter, R_q (μm) is the root-mean-square (rms) roughness and the waviness parameter, W_q (μm), is the root-mean-square (rms) waviness. Thus, they are defined as the average of the measured height deviations taken within the evaluation length or area and measured from the mean linear surface (Eq. 1). $Z(x)$ represents the height elements along the profile and L is the number of discrete elements.

$$\text{rms} = \sqrt{\frac{1}{L}\int_0^1 z^2(x)\mathrm{d}x} \quad (\mu\text{m}) \tag{1}$$

Through a digital filtering (cutoff filter) of the data, the surface characteristics of the investigated surface can be broken down into waviness and roughness results. This filter includes a high filter wavelength which defines the noise threshold; all shorter spatial wavelengths are considered noise. It also includes a low filter wavelength which defines the form threshold where all longer spatial wavelengths are considered form (waviness). Everything

between these two wavelengths is assigned to roughness. Also in this case it is essential that the choice of reference values is well considered.

Experimental Setup, Sampling and Data Analysis

Each sample was fixed to a microscope slide, which was fitted into a 90° angle on a rectangular plate. This plate was mounted on the profilometry stage with screws and was thereby fixed in the same position on each occasion. The different analysis points had known *x*- and *y*-coordinates, and by means of these coordinates the different analysis points could be retrieved. In this study a 20× Mirau interference objective (Zygo) with a 1× zoom was used, which provide an image of 350 × 263 μm, with a theoretical lateral resolution of 0.88 μm. By using the lab-made mounting we were able to analyze the same area (±20 μm) on each analysis occasion. This enabled us to follow and compare surface changes in that specific area of interest. As a result, we were able to reduce noise, normally observed due to the use of different spots for data collection.

Sampling was performed when the samples were received, i.e. week 0, and then after storage of 2, 4, 12 and 36 weeks, respectively. Three samples from the cycled temperature conditions were monitored, and measurements were carried out at three different spots for each sample. Since the constant temperature was set as a reference temperature, one sample from this environment was analyzed. Also here measurements were carried out at three different spots. The analyses were performed on the top of the pralines, at room temperature (20 °C approximately). After each measurement the samples were put back into their temperature-controlled environment for continued storage.

The data was analyzed using the advanced texture application in MetroPro™ (Middlefield, CT, USA) analysis and control software. Roughness (R_q), waviness (W_q), peak number, peak height and peak area were investigated in this study. The reference band for peak definition was set at 2 μm. The cutoff filter, defining roughness and waviness, were set at 1.5 and 100 μm, respectively, which give a high filter frequency of 0.67 μm^{-1} and a low filter frequency of 0.01 μm^{-1}.

Low Vacuum Scanning Electron Microscopy

Scanning electron microscopy (SEM) is a technique producing high resolution images of a sample surfaces. Due to the way in which the image is created, SEM images have a characteristic three-dimensional appearance and are useful for judging the surface structure of a sample. A Philips XL30 environmental scanning electron microscope, equipped with a cold stage set to 5 °C was used with mixed detectors [biased gaseous detector (GSE) 75% and back-scattered electron detector (BSE) 25%], at 15 keV and in the low vacuum mode with 0.7–0.9 Torr, which gives an RH of 13% approximately. These parameters were chosen considering that they cause minimal damage of the chocolate surface, and for optimizing the imaging quality. In this study, analyses of the samples were performed without sample preparation, i.e. without coating the sample surface. This leads to a sacrifice in magnification and resolution; however, by analyzing without a coating, the true surface can be monitored.

Sampling was performed parallel to profilometry, meaning when the samples were received, i.e. week 0, and then after storage of 2, 4, 12 and 36 weeks, respectively. Two samples from each environment were monitored on each analysis occasion, and the analysis was performed on the top of the pralines, as for profilometry. After each analysis the monitored samples were sacrificed due to the possible impact from the microscope such as electron beam, temperature, humidity and pressure.

Results and Discussion

Macroscopic Observations

The samples stored at a cycled temperature developed a soft shell and a visually observed hardened filling, after 36 weeks of storage. These shells also expanded by 2 mm in diameter (7%) compared to the fresh samples and the samples stored at a constant temperature. At the same time, the volume of the filling decreased markedly and the bottom of the praline cracked and moved towards the center of the praline (Fig. 1). The temperature fluctuations in the cycled environment probably led to liquid TAG moving from the filling into the shell of the praline, giving an expansion of the shell and shrinkage of the filling. As a consequence of the change in composition we expect the shell to become softer and the filling to become harder. Further, the water activity in the filling was measured to a value of 0.77. Therefore, it could be suggested that diffusion of moisture from the filling into the shell led to swelling of milk particles, which simultaneously to the fat migration caused swelling of the shell and a decrease in filling volume [20, 35]. In addition, the glossiness of the cycled samples disappeared and its color turned to white compared to creamy white for the fresh samples, which could be described as visible bloom development. Further, the presence of moisture in the filling could lead to sugar bloom development in addition to fat bloom development.

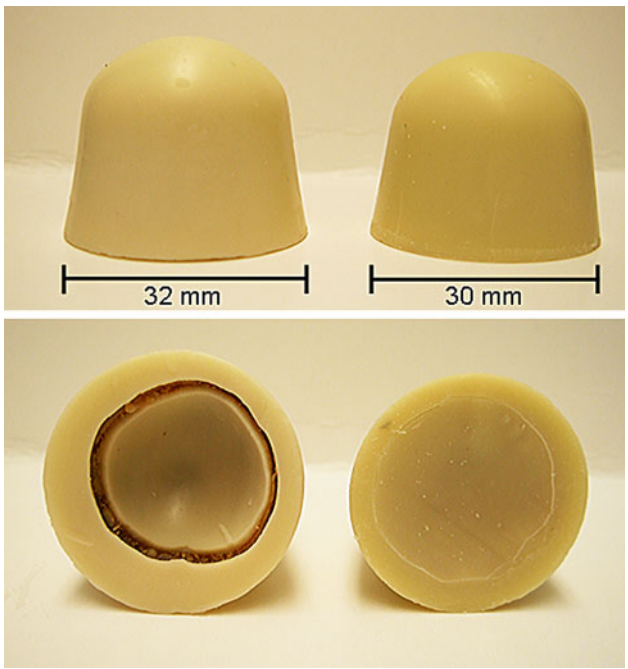

Fig. 1 White chocolate praline from the front and from underneath. *Left* sample stored at a cycled temperature, after 36 weeks. *Right* sample stored at a constant temperature, after 36 weeks

Microscopic Observations

Samples Stored at a Constant Temperature of 18 °C

The profilometry and LV SEM results in Fig. 2 demonstrates how the surface topology and the topological features change over time, i.e. from week 0 to week 36, when stored at a constant temperature. The surface images to the left represent 2D profilometry images (350 × 263 μm), and to the right LV SEM images are displayed in the same size range as the profilometry images. It should be noted that the profilometry images are produced from the same spot on the same samples, while all the LV SEM images represent different samples, and hence larger surface variability is to be expected from the latter method. However, the result images from both profilometry and LV SEM are representative.

Some profilometry data are not interpretable due to the method's detection limit, with regards to topological features with high inclinations (>15°). This is illustrated by a black color in the images. Table 2 shows the mean number of points per observation area at each analysis occasion, which displays values that give the information of data drop out. Further, the number of points for samples stored at a constant temperature at week 36 is too low ($113 \times 10^3 \pm 8.7$ points per observation area) to be able to use for interpretation of the data, this probably due to high inclinations of the topological features.

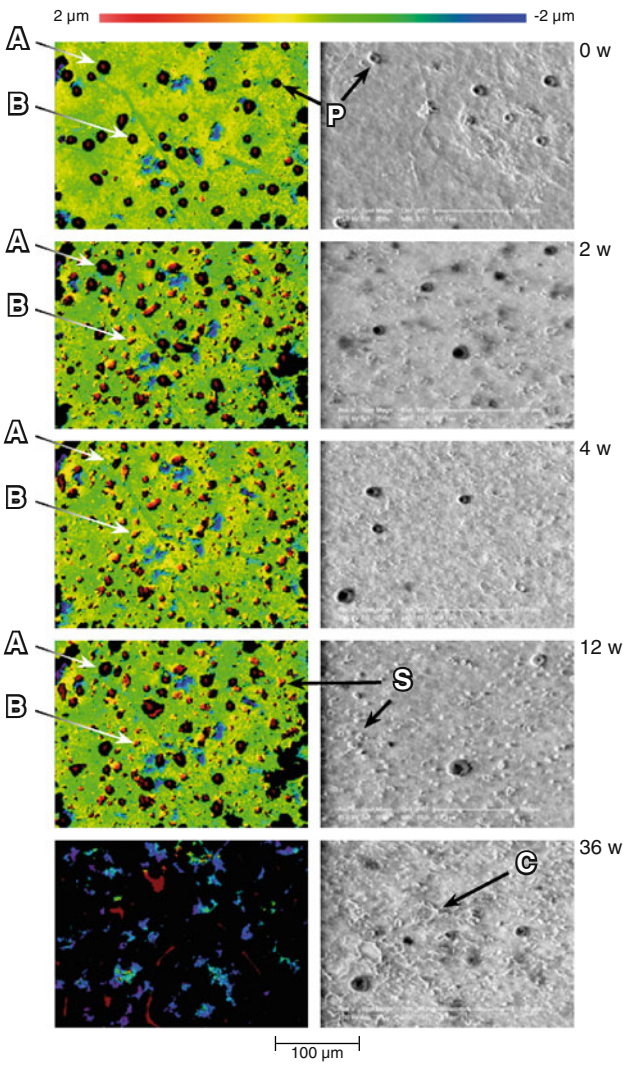

Fig. 2 Surface images of white chocolate pralines stored at a constant temperature (18 °C). *Left* 2D profilometry images (350 × 263 μm), produced from the same spot on the same sample, weeks 0, 2, 4, 12, 36. Some of the protrusions disappear and then re-appear (*A*), while some change their appearance over time (*B*). *Right* LV SEM images, from different samples, weeks 0, 2, 4, 12, 36, including protrusions (*P*), ridge-like topological features (*S*) and needle-shaped crystals (***C***)

As can be concluded from these images, the changes of the surface topology show similar appearance over time by using both profilometry and LV SEM. At week 0 both methods indicate a surface with a fine roughness, including protrusions (mountain-like topological features) with sharp inclinations heterogeneously spread over the surface, and with a size range of a few microns to around 20 μ in diameter. After 2 weeks of storage only few of these protrusions remain. Further, the images from both techniques illustrate additional ridge-like topological features with a wide size range, of different shapes and less sharp inclinations. After 4 weeks of storage, the surface is

Table 2 Number of points per observation area (350 × 263 μm) and standard error of mean for each profilometer analyze occasion of white chocolate pralines stored at 18 °C and at 15–25 °C, respectively (maximum number of points = 307 × 10^3)

Week	Cycled temperature (%)	Sem[a] cycled temperature (%)	Constant temperature (%)	Sem[a] constant temperature (%)
0	87	1.2	85	2.4
2	95	1.1	71	4.2
4	96	0.8	85	1.6
12	90	1.4	76	2.4
36	83	1.7	37	2.8

[a] Standard error of mean

homogeneously covered by these new ridge-like topological features, and after 12 weeks of storage both types of topological features mentioned are present. Further, the LV SEM images show a surface with more distinct topological features at week 12 compared to week 2 and 4. Since it is always the same area that is analyzed by the profilometer, it can be noted that some of the protrusions disappear and some reappear over time (point A and B in Fig. 2), at the same time as new topological features arise at the surface. After 36 weeks of storage, LV SEM images show that the surface is completely dominated by different topological features, some of them observed as needle-like shapes. The profilometry images show a large number of lost data, most likely due to a very rough surface.

In order to ensure that the surface topological features resembling protrusions actually are protrusions, sample surfaces were monitored by LV SEM from a tilted angle. These results, which are represented in Fig. 3, show that the surface displays protrusions of various sizes.

The result parameter peak height (μm), for samples stored at a constant temperature, is illustrated in Fig. 4. These results indicate that the low frequency of peaks present at week 0 is in the height range of 1–6 μm. Further, between week 0 and 2, the frequency of smaller peaks (<3 μm) has increased markedly in number, after which the number remains nearly constant. In addition, the frequency of larger peaks is higher by week 2 and 12. In Fig. 5 the parameter peak area (μm^2) is shown for samples stored at a constant temperature. At week 0 the results indicate that there is a small number of peaks, and that these peaks are spread over a wide size range. Between week 0 and 2, an increase in the number of peaks can be observed, and these peaks show an even wider size distribution. These results correlate with the profilometry images and the LV SEM images in Fig. 2, where new shapes of surface imperfections, with a wide size distribution appear by week 2 and stay until week 12. In addition to these topological features, larger mountain-like protrusions are present at week 2 and 12.

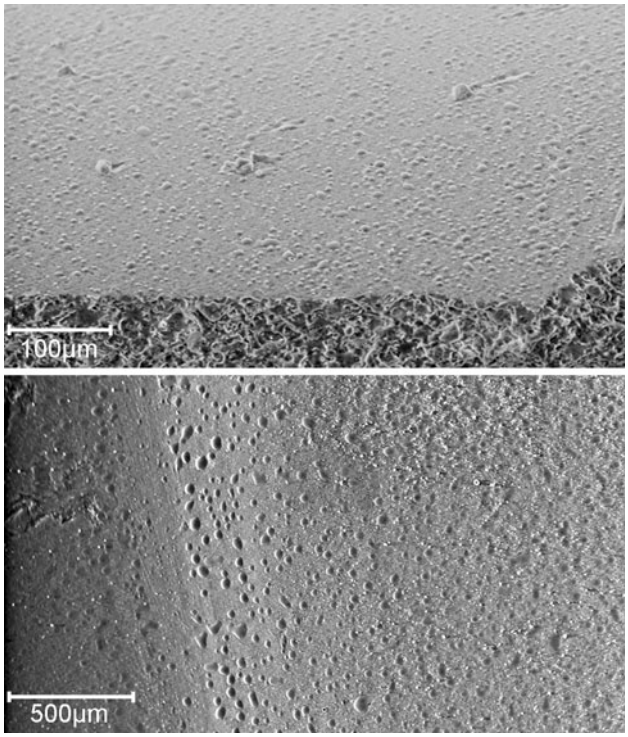

Fig. 3 LV SEM images of tilted chocolate samples

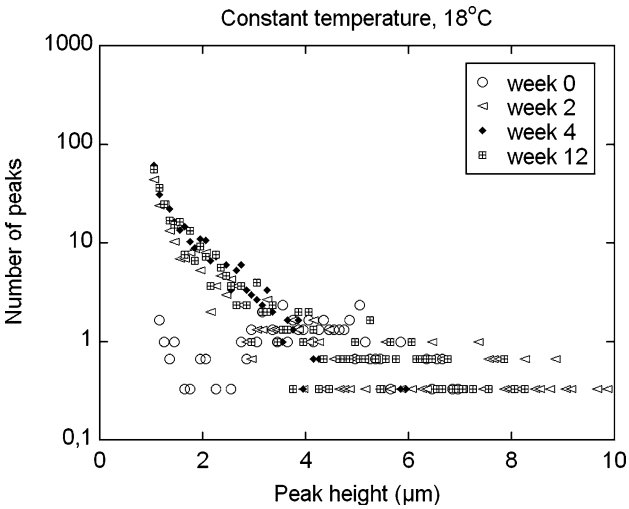

Fig. 4 Number of peaks per observation area (350 × 263 μm) as a function of peak height for samples stored at a constant temperature (18 °C). The number is calculated as a mean of $n = 3$. The standard error of mean is ±0.9

Samples Stored at a Cycled Temperature, 15–25 °C

Development of the topological surface features of samples stored at a cycled temperature (15–25 °C), investigated using profilometry and LV-SEM, is shown in Fig. 6. At week 0 the results show protrusions with sharp inclinations heterogeneously spread over the surface, and with a size

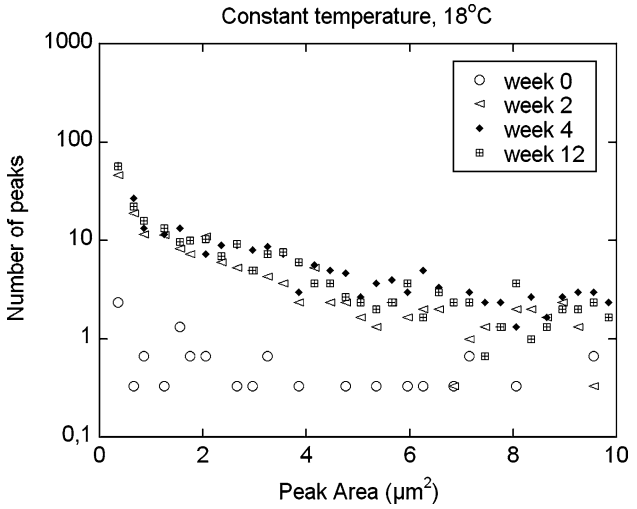

Fig. 5 Number of peaks per observation area (350 × 263 μm) as a function of peak area for samples stored at a constant temperature (18 °C). The number is calculated as a mean of $n = 3$. The standard error of mean is ±1.2

range of a few microns up to around 20 μ in diameter. After 2 weeks of storage the surface appears relatively smooth, and the protrusions from week 0 have generally disappeared. The surface remains almost similar after 4 weeks of storage, and after 12 weeks a homogeneously rough surface is observed that evolves to be even rougher after 36 weeks of storage (note that between week 12 and 36, the samples were stored at 18 °C), although with less height variation compared to the constant temperature samples. As indicated by point A in Fig. 6, some topological features disappear completely, while others remain throughout the storage period and become enhanced with time (point B in Fig. 6). The roughness is created by comparable smooth ridges, particularly visible in the LV SEM images, at week 12 and 36. A comparable morphology is not observable in the samples stored at a constant temperature.

Figure 7 shows the frequency as a function of peak height (μm) for samples stored at a cycled temperature. These results show that the larger peaks (2–6 μm) almost disappear from week 0 to week 2, reach a minimum week 2–4, and increase again between week 12 and 36 (2–4 μm). The sharp peaks between 4 and 6 μm do not return. Further, from week 4 to week 12 and 36 a sharp increase in frequency of smaller peaks (<2 μm) can be observed. The development of the frequency as a function of peak area (μm^2) is shown in Fig. 8. The results show that over time the sample surfaces develop many small peaks, in the size range of 1–2 μm^2, and with a dominant peak area of <1 μm^2. After 2 and 4 weeks a decrease in the frequency of larger peaks with an area between 2 and 8 μm^2 can be observed. At longer times, 12–36 weeks, an increase in all

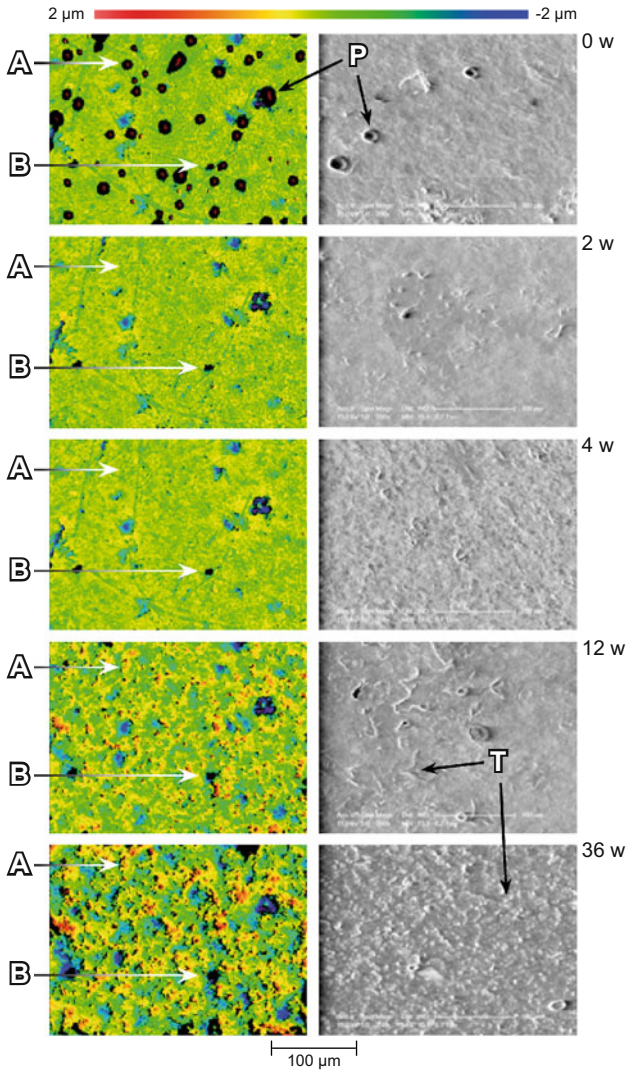

Fig. 6 Surface images of white chocolate pralines stored at a cycled temperature (15–25 °C). *Left* 2D profilometry images (350 × 263 μm), produced from the same spot on the same sample, week 0, 2, 4, 12, 36. Some surface topological features disappear completely over time (*A*), while some remain and become enhanced with time (*B*). *Right* LV SEM images, from different samples, week 0, 2, 4, 12, 36, including protrusions (*P*) and other topological features (*T*)

size ranges is observed. These results are consistent with the images in Fig. 6, which show a presence of relatively large protrusions at week 0, and then a development of topological features of various sizes from week 2 to 36.

Quantitative Analysis by Peak Number (Peaks per Observation Area)

The mean peak number per observation area (350 × 263 μm) as a function of time for samples stored at constant and at cycled temperature, respectively, is shown in Fig. 9. The results of the samples stored at 18 °C show a

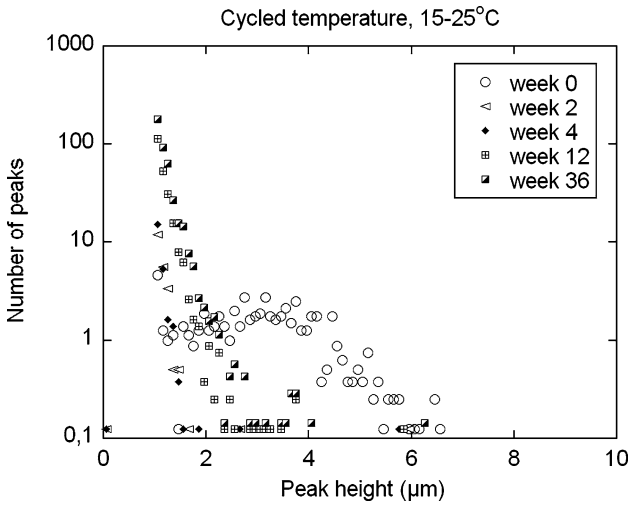

Fig. 7 Number of peaks per observation area (350 × 263 μm) as a function of peak height for samples stored at a cycled temperature (15–25 °C). The number is calculated as a mean of $n = 9$. The standard error of mean is ±1.0

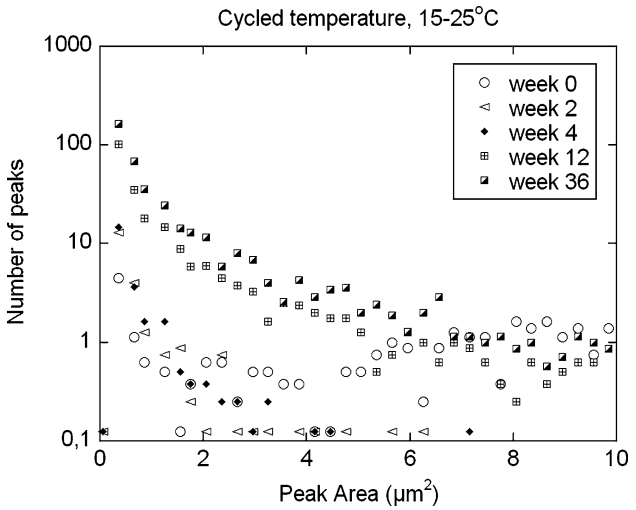

Fig. 8 Number of peaks per observation area (350 × 263 μm) as a function of peak area for samples stored at a cycled temperature (15–25 °C). The number is calculated as a mean of $n = 9$. The standard error of mean is ±0.9

sharp rise in peak number from week 0 to week 2 and 4 (From 49 to 290 peaks per observation area), which then remains steady until week 12. The sharp increase from week 0 to week 2 also agrees with the impression in Fig. 2, where new topological features have developed after 2 weeks. In contrast to the samples stored at a constant temperature, the peak number for the cycled samples decreases from week 0 to week 2 (from 62 to 25 peaks per observation area) and then remains stable until week 4. Further on, between week 4 and 12, a sharp increase in peak number can be observed (from 24 to 270 peaks per observation area), which continues until week 36 (420

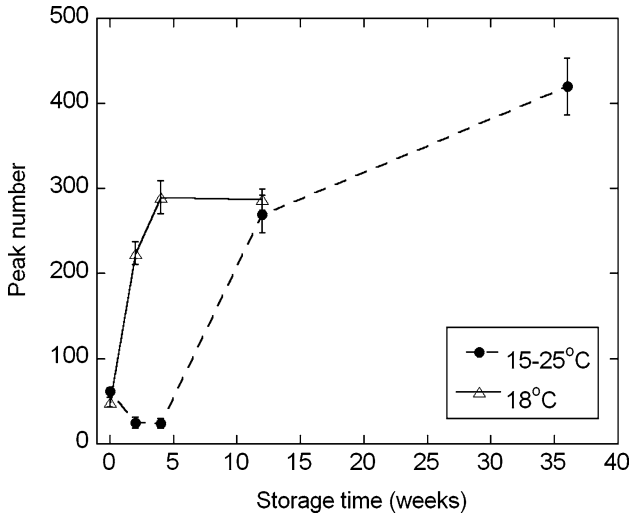

Fig. 9 Number of peaks (1–10 μm) per observation area (350 × 263 μm) as a function of time for samples stored at 18 °C (*open triangles*) and at 15–25 °C (*filled circles*), respectively. The *error bars* show the standard error of mean

peaks per observation area). Also these results can be correlated to the images in Fig. 6, where the surface appears relatively smooth at week 2 and 4, and then an increase in irregularities at the surface during week 12 and 36 can be observed. In addition, the peak number is within the same order of magnitude (approximately 50 peaks per observation area) at week 0 for all samples, which suggests that the samples possessed a similar surface appearance prior to storage at different temperature conditions.

Quantitative Analysis by Roughness, R_q (μm), and Waviness, W_q (μm)

The roughness, R_q, is presented as a function of time in Fig. 10. For the samples stored at a constant temperature, the roughness increases from week 0 to week 2 (from 0.5 to 0.8 μm) and then decreases to a value (0.5 μm) close to the starting value. After week 4 the roughness increases again (to a value of 0.7 μm). These roughness results can further be connected to the surface images in Fig. 2, where an increase in quantity of surface imperfections can be observed at week 2. Then, at week 4, the protrusions observed at week 0, disappear which would give a decrease in roughness. Some of these protrusions then reappear at week 12, where we also see an increase in roughness. On the other hand, R_q values for samples stored at a cycled temperature behave similar to the peak number, where we at first can observe a decrease in roughness, and then after week 4 an increase. This similar behavior is probably due to the fact that there are no protrusions observed after week 0. Thus, also R_q for the cycled samples can be connected to the images in Fig. 6. Further, the R_q values lie within the

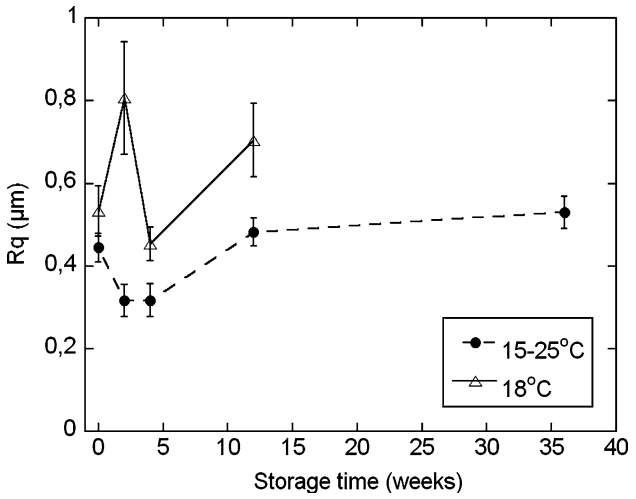

Fig. 10 R_q as a function of time for samples stored at 18 °C (*open triangles*) and at 15–25 °C (*filled circles*), respectively, including standard error of mean

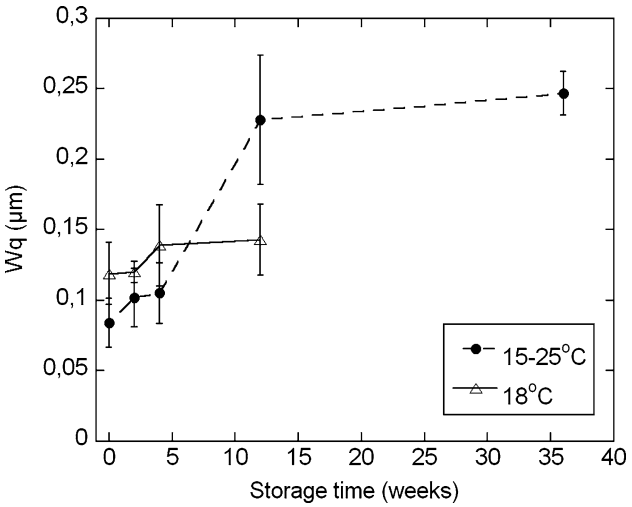

Fig. 11 W_q as a function of time for samples stored at 18 °C (*open triangles*) and at 15–25 °C (*filled circles*), respectively, including standard error of mean

same order of magnitude (around 0.5 µm) at week 0 for all samples. Thus, the samples displayed a similar roughness prior to the distribution into different storage conditions.

Figure 11 presents the waviness, W_q, as a function of time for samples stored at a constant and a cycled temperature, respectively. Both results indicate an increase from week 0. Still, for the cycled samples the inclination is steeper between week 4 and 12 than for the samples stored at a constant temperature ($\Delta W_{q\ \text{cycled}} = 0.12$ µm and $\Delta W_{q\ \text{constant}} = 0.03$ µm). This can be connected to the profilometry images in Fig. 6, where there is a distinct difference between week 4 and 12 in means of large irregularities. In contrary, the overall waviness does not seem to vary to any great extent in the images in Fig. 2.

Discussion

The results presented in Fig. 2 show that the pralines stored at a constant temperature for 2 weeks display large protrusions (as evident in Fig. 3) that are gradually changing into ridge-like structures. The smooth nature of the protrusions suggests that these topological features consist of oil (i.e. are not crystallized), from the filling and the chocolate matrix, that has been transported to the surface of the chocolate. A convective flow of this type, spreading at the surface, is probably caused by a pressure gradient. In the case of samples stored at a constant temperature (18 °C), the chocolate contracts due to crystallization. As there is more liquid fat in the filling than in the shell, the shell contracts more than the filling. This would lead to a higher internal pressure that may press liquid fat to the surface. Further, we suggest that the bloom development is a two-step process (pores to oil-filled protrusions to crystals), with the mentioned protrusions initially forming at the surface and then crystals nucleating and growing from them. Thus, the developed ridge-like features are most likely to be interpreted as an early sign of crystallization, and hence indicative for future bloom development. These suggestions are supported by the quantitative data, where the number of small peaks (Fig. 4) increases with time rapidly in the first 2 weeks and the number of larger peaks increases more gradually (Fig. 5). Further there is a wide size distribution of the peaks (Fig. 5). These observations and suggestions agree well with earlier studies observing conical protrusions acting as sites for crystal growth and chocolate bloom [27, 28].

The possibility of sugar bloom formation is also to be considered. However, since some of the ridge-like features seem to be connected to the original protrusions we suggest that these features consist of fat.

The results presented in Fig. 6 show that the pralines stored at a cycled temperature after 2 weeks become smoother, in contrast to the samples at the constant temperature. Very few structures are observed in the microscope although an increase in very small peaks is observed (Figs. 7, 8). After a longer time, more shallow waves are observed, an increased number of smaller peaks with a large area and increased waviness (Fig. 11). The filling shrinks and the shell expands according to the measured macroscopic shape. Thus, we may assume that we might have a flux of oil from the filling into the shell but to a lesser extent to the surface. The early observations of protrusions are most likely caused by a convective flow, due to a pressure gradient originating from the shrinking when the praline was formed. In this case of samples stored at a cycled temperature, the temperature fluctuations should lead to periodic changes in solid fat content (SFC).

Further, temperature gradients arise within the chocolate sample, a warmer surface when the temperature is increased and a warmer interior when the temperature is decreased. This would lead to an overpressure in the filling during cooling and an under pressure during heating. Thus, protrusions formed in the cooling cycle can be sucked into the structure in the heating cycle. Therefore, volume changes and pressure fluctuations would occur. Thus, it may be concluded that the main mechanism taking place in this case could be due to the fluctuation of the internal pressure (which is due to the change in SFC), where liquid fat is moving in two directions, i.e. pushed through the chocolate shell and up to the surface and also reabsorbed back into the chocolate shell [1, 11, 13]. However, as can be seen in Fig. 1, the bottom of the praline eventually cracked and moved towards the center of the praline. This is probably an effect of the pressure differential, and as the cracks appear the pressure differences should be equalized.

Some of the liquid fat that has been transported to the surface may spread out over the surface and give rise to a smoothening effect. Over time this liquid fat at the surface could allow movement of the solid components (solid fat crystals, sugar, milk solids, etc.) [12, 13], giving rise to the surface topology that can be observed at week 12 and 36 in Fig. 6. This can further be supported by the development of peak number and R_q, and also by the peak height and peak area results, which indicate an increase in amount of small peaks, but also larger, shallow peaks over time.

The developed waviness, which has increased markedly by week 12, may be interpreted as an effect of internal crystal changes in the chocolate shell. As the composition of the shell matrix changes, as a consequence of absorption of filling fat, it will be more susceptible to re-crystallization. Further support for this crystal growth within the matrix comes from the observations of the nature of the surface topology in the images after 12 and 36 weeks (Fig. 6).

The roughness and the number of peaks were consistently higher for the samples stored at a constant temperature than for the samples stored in a cycled environment, while the waviness developed higher values for the cycled samples. The LV SEM images from the samples stored at a constant temperature showed, among other topological structures, some needle-like crystals at the surface after 36 weeks of storage. This was not the case for the samples stored in a cycled environment, but instead other types of topological structures were observed. The lack of needle-like fat bloom crystals on the cycled samples could be due to the high temperature during cycling. Thus, the fat bloom crystal development could be connected to the higher values of roughness and peak number, while the swelling and reorganization of the chocolate matrix could be connected to the higher waviness values. Since the samples were white, the development of visual bloom was impossible to determine. Still, after 36 weeks the cycled samples appeared whiter than the samples stored at a constant temperature. Thus, this color change would not be due to developed fat bloom crystals, but rather to other surface changes which are reflecting changes within the chocolate matrix.

Since the migrating oil wells out at the surface, it may be concluded that capillary flow is not the mechanism connected to the protrusions in these studies. In the case of capillary flow [19–21] the oil would stop at the surface level. Still, capillary flow could be an additional mechanism present, contributing to the absorption of oil into the shell.

Conclusion

This study demonstrates that the surface topology development over time can be conveniently followed in a specific area, by using profilometry, both quantitatively and qualitatively. Further, the combined information from profilometry and LV SEM can after validation provide an analytical toolkit for the early recognition of surface changes and hence early bloom development in the process of chocolate manufacture and storage. Further, distinct differences in surface topology development could be observed between samples stored in two different environments regarding macroscopic and microscopic information, and regarding qualitative and quantitative data, which all support each other. The statistical quantification of the images shows that the degree of surface roughness increases with time in terms of peak number, roughness, waviness, peak height and peak area for both storage environments, still with diverse magnitude and velocity. Since the surface development was followed in the same area of interest, the change of specific topological features over time could be monitored and thus, together with the statistical parameters, give more information to possible mechanisms of fat migration. The results suggest that some imperfections, in form of pores or protrusions, could play a role in the development of fat bloom, and that there may be different main mechanisms of fat migration taking place depending on the storage conditions. Regarding the samples stored at a constant temperature we suggest a convective flow as a main mechanism, where a two-step process could take place, with oil protrusions initially forming at the surface and then crystals nucleating and growing from them. In the case of storage at a cycled temperature there is a decrease in the filling volume, probably caused by a migration of liquid fat from the filling into the expanding shell. In addition our observations show an effect which can be interpreted as a convective flow through pores and cracks in two directions, i.e. up to the surface and back into the shell. The driving internal pressure fluctuations may be due to changes in the liquid to

solid ratio in the fat at the surface and internally when the temperature is cycled. Part of the liquid fat could be pressed out at the surface, spreading out, allowing movement of the solid components, while part of the liquid fat could be reabsorbed into the chocolate shell, where re-crystallization could occur.

Through this study a positive correlation of profilometry data to early chocolate bloom development has been established on white chocolate samples. Further work needs to be undertaken, and is in progress, for the early prediction of visible fat bloom and not only the monitoring of early fat bloom development.

Acknowledgments This work was funded by the EU commission, grant 218423 under FP7-SME-2007-2, project officer German Valcárcel (German.Valcarcel@ec.europa.eu). The authors thank Ganache AB for providing the chocolate samples, and for valuable input from other partners of the ProPraline project. Further we thank Rodrigo Robinson and Mikael Sundin for providing valuable support and helpful information.

References

1. Lonchampt P, Hartel RW (2004) Fat bloom in chocolate and compound coatings. Eur J Lipid Sci Technol 106:241–274
2. Padar S, Jeelani SAK, Windhab EJ (2008) Crystallization kinetics of cocoa fat systems: experiments and modeling. J Am Oil Chem Soc 85:1115–1126
3. Wille R, Lutton E (1966) Polymorphism of cocoa butter. J Am Oil Chem Soc 43:491–496
4. Larsson K (1966) Classification of glyceride crystal forms. Acta Chem Scand 20:2255–2260
5. van Malssen K, van Langevelde A, Peschar R, Schenk H (1999) Phase behavior and extended phase scheme of static cocoa butter investigated with real-time X-ray powder diffraction. J Am Oil Chem Soc 76:669–676
6. Schenk H, Peschar R (2004) Understanding the structure of chocolate. Radiat Phys chem 71:829–835
7. Yano J, Ueno S, Sato K, Arishima T, Sagi N, Kaneko F, Kobayashi M (1993) FT-IR study of polymorphic transformations in SOS, POP, and POP. J Phys Chem 97:12967–12973
8. van Mechelen Jan B, Goubitz K, Pop M, Peschar R, Schenk H (2008) Structures of mono-unsaturated triacylglycerols. V. The β'1–2, β'-3 and β2–3 polymorphs of 1, 3-dilauroyl-2-oleoylglycerol (LaOLa) from synchrotron and laboratory powder diffraction data. Acta Crystallogr Sect B Struct Sci 64:771–779
9. Lohman MH, Hartel RW (1994) Effect of milk fat fractions on fat bloom in dark chocolate. J Am Oil Chem Soc 71:267–276
10. Kinta Y, Hatta T (2007) Composition, structure, and color of fat bloom due to the partial liquefaction of fat in dark chocolate. J Am Oil Chem Soc 84:107–115
11. Hartell RW (1999) Chocolate: fat bloom during storage. Manuf Confect 79(5):89–99
12. James BJ, Smith BG (2009) Surface structure and composition of fresh and bloomed chocolate analysed using X-ray photoelectron spectroscopy, cryo-scanning electron microscopy and environmental scanning electron microscopy. LWT Food Sci Technol 42:929–937
13. Hodge SM, Rousseau D (2002) Fat bloom formation and characterization in milk chocolate observed by atomic force microscopy. J Am Oil Chem Soc 79:1115–1121
14. Smith KW, Cain FW, Talbot G (2007) Effect of nut oil migration on polymorphic transformation in a model system. Food Chem 102:656–663
15. Depypere F, De Clercq N, Segers M, Lewille B, Dewettinck K (2009) Triacylglycerol migration and bloom in filled chocolates: effects of low-temperature storage. Eur J Lipid Sci Technol 111:280–289
16. Miquel ME, Carli S, Couzens PJ, Wille HJ, Hall LD (2001) Kinetics of the migration of lipids in composite chocolate measured by magnetic resonance imaging. Food Res Int 34:773–781
17. Ghosh V, Ziegler GR, Anantheswaran RC (2002) Fat, moisture, and ethanol migration through chocolates and confectionary coatings. Crit Rev Food Sci Nutr 42:583–626
18. Löfborg N, Smith P, Furó I, Bergenståhl B (2003) Molecular exchange in thermal equilibrium between dissolved and crystalline tripalmitin by NMR. J Am Oil Chem Soc 80:1187–1192
19. Marty S, Baker K, Dibildox-Alvarado E, Rodrigues JN, Marangoni AG (2005) Monitoring and quantifying of oil migration in cocoa butter using a flatbed scanner and fluorescence light microscopy. Food Res Int 38:1189–1197
20. Choi YJ, McCarthy KL, McCarthy MJ, Kim MH (2007) Oil migration in chocolate. Appl Magn Reson 32:205–220
21. Aguilera JM, Michel M, Mayor G (2004) Fat migration in chocolate: diffusion or capillary flow in a particulate solid? A hypothesis paper. J Food Sci 69:R167–R174
22. Briones V (2006) Scale-sensitive fractal analysis of the surface roughness of bloomed chocolate. J Am Oil Chem Soc 83:193–199
23. Briones V, Aguilera JM, Brown C (2006) Effect of surface topography on color and gloss of chocolate samples. J Food Eng 77:776–783
24. Rousseau D (2006) On the porous mesostructure of milk chocolate viewed with atomic force microscopy. Food Sci Technol 39:852–860
25. Rousseau D, Smith P (2008) Microstructure of fat bloom development in plain and filled chocolate confections. Soft Matter 4:1706–1712
26. Rousseau D, Sonwai S (2008) Influence of the dispersed particulate in chocolate on cocoa butter microstructure and fat crystal growth during storage. Food Biophys 3:273–278
27. Smith PR, Dahlman A (2005) The use of atomic force microscopy to measure the formation and development of chocolate bloom in pralines. J Am Oil Chem Soc 82:165–168
28. Sonwai S, Rousseau D (2008) Fat crystal growth and microstructural evolution in industrial milk chocolate. Cryst Growth Des 8:3165–3174
29. Loisel C, Lecq G, Ponchel G, Keller G, Ollivon M (1997) Fat bloom and chocolate structure studied by mercury porosimetry. J Food Sci 62:781–788
30. Grove GL, Grove MJ, Leyden JJ (1989) Optical profilometry: an objective method for quantification of facial wrinkles. J Am Acad Dermatol 21:631–637
31. Cross SE, Kreth J, Wali RP, Sullivan R, Shi W, Gimzewski JK (2009) Evaluation of bacteria-induced enamel demineralization using optical profilometry. Dent Mater 25:1517–1526
32. Visscher M, Hendriks CP, Struik KG (1994) Optical profilometry and its application to mechanically inaccessible surfaces. Part II. Application to elastometer/glass contacts. Precis Eng 16:199–204
33. Thomas TR (1999) Rough surfaces, 2nd edn. Imperial College Press, London
34. ZygoCorporation (1998) MetroPro reference guide, Middlefield, Connecticut
35. Ghosh V, Ziegler GR, Anantheswaran RC (2005) Moisture migration through chocolate-flavored confectionery coatings. J Food Eng 66:177–186